ELSEVIER

Catalysis Today 59 (2000) 141–150

CATALYSIS TODAY

www.elsevier.com/locate/cattod

Hydrogen assisted catalytic combustion of methane on platinum

O. Deutschmann[a,*], L.I. Maier[a], U. Riedel[a], A.H. Stroemman[b], R.W. Dibble[b,1]

[a] *IWR, Universität Heidelberg, Im Neuenheimer Feld 368, D-69120 Heidelberg, Germany*

[b] *Department of Mechanical Engineering, University of California, Berkeley, CA 94720, USA*

Abstract

The objective of this paper is to study hydrogen assisted catalytic combustion of methane on platinum experimentally and numerically. In the experiment, we measure the exit temperatures of methane/hydrogen/air mixtures flowing at atmospheric pressure through platinum coated honeycomb channels. A single channel of this monolith is investigated numerically by a two-dimensional Navier–Stokes simulation including an elementary-step surface reaction mechanism. Furthermore, a one-dimensional time-dependent simulation of a stagnation flow configuration is performed to elucidate the elementary processes occurring during catalytic ignition in the mixtures studied. The dependence of the hydrogen assisted light-off of methane on hydrogen and on methane concentrations is discussed. The light-off is primarily determined by the catalyst temperature that is a result of the heat release due to catalytic hydrogen oxidation. Increasing hydrogen addition ensures light-off, decreasing hydrogen addition requires an increasing methane feed for light-off.

Keywords: Catalytic combustion; Numerical simulation; Reaction kinetics; Catalytic ignition

1. Introduction

The application of catalytic combustion in gas turbines critically depends on the feasibility of a convenient light-off mechanism of the catalytic combustor, because ignition of methane on platinum and palladium occurs at relatively high temperatures at lean conditions [1,2]. The addition of hydrogen to the initial mixture may help to reduce the ignition temperature, because ignition of hydrogen on platinum occurs at almost room temperature. In the present work, the hydrogen assisted catalytic ignition of lean methane/air mixtures on platinum is studied experimentally and numerically.

In the experiment, methane/hydrogen/air mixtures flow through platinum coated honeycomb monoliths. The exit temperature is monitored as a function of methane and hydrogen concentration. Each experimental run starts with a pure hydrogen/air flow that is ignited catalytically. Then, the methane feed is slowly increased. Depending on hydrogen as well as methane inlet concentrations, hydrogen or both hydrogen and methane are oxidized catalytically.

Numerical simulations are performed for two configurations, the stagnation point flow onto a platinum foil and the flow through a single channel of the honeycomb monolith. In both systems, detailed models for transport and surface chemistry are used. The stagnation flow system is described by a one-dimensional simulation, where the distance from the foil and the time are the independent variables. Since this code is

* Corresponding author. Tel.: +49-6221-54-8886; fax: +49-6221-54-8884.

E-mail addresses: deutschmann@iwr.uni-heidelberg.de (O. Deutschmann), rdibble@firebug.me.berkely.edu (R.W. Dibble)

[1] Tel.: +1-510-642-4901; fax: +1-510-642-1850.

0920-5861/00/$ – see front matter
PII: S0920-5861(00)00279-0

able to simulate transient problems, it is used to understand the behavior during ignition processes. The single channel flow is studied by a two-dimensional, axi-symmetric simulation of the Navier–Stokes equations. This approach permits to study the interaction of transport, surface chemistry, and heat transfer in the honeycomb channels.

2. Experimental studies

2.1. Experimental setup

A sketch of the experimental setup is shown in Fig. 1. A 5.0 cm diameter flow reactor contains two thermally insulated honeycomb monoliths, 2.5 cm in length each. The features of the monoliths are: alumina washcoat of 0.16 g alumina per 1 g cordierite substrate, platinum loading of 0.01 g per 1 g substrate, 200 cells per square inch with 20% blockage resulting in a single channel diameter of approximately 1.8 mm. The inflow is varied between 66 and 216 slpm air with various hydrogen and methane additions. The inlet mixture is at room temperature and at atmospheric pressure. The outlet temperature (T_{out}) is measured directly behind the monolith exit on the centerline of the reactor using a thermocouple.

2.2. Experimental results

Each experimental run starts with a pure constant hydrogen/air flow that is ignited catalytically. All the hydrogen is consumed by heterogeneous reactions

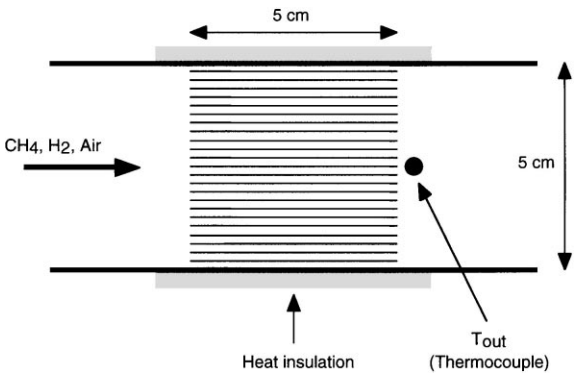

Fig. 1. Sketch of the experimental setup.

on the catalytic platinum coating. Adding additional lengths of catalyst did not change the outlet temperature. The temperature of the inlet gas of 300 K is increased rapidly inside the reactor due to the high exothermic oxidation reaction. The resulting monolith temperature is between 600 and 720 K depending on the hydrogen feed between 4.25 and 6.0 vol.%. This temperature is measured directly behind the monolith in the gas phase. Because of heat losses from the monolith to the ambient room temperature and a possible temperature decrease in the gas between monolith and thermocouple, which cannot be prevented using the current equipment, the measured temperature is approximately 100 K less than that the adiabatic temperature would be for complete hydrogen consumption.

After the hydrogen/air flow is ignited, the methane flow is slowly increased. Fig. 2 shows the experimental measured outlet temperatures as function of methane feed for several initial hydrogen concentrations which are kept constant during a run (curve). Almost no temperature variation is observed for low hydrogen concentrations below 4.25 vol.%. Even when the methane feed is increased to over 6%, being within the flammability limit of methane/air mixtures, the temperature stays constant. Hence, no methane is consumed; catalytic methane combustion is not ignited. The catalyst temperature seems to be too low to lead to light-off. A more detailed discussion of this behavior will be given in Section 4.

At hydrogen feed above 4.75 vol.%, a temperature jump occurs at a sufficiently high methane concentration. For example at 4.75 vol.% H_2, the temperature suddenly increases from 660 to over 1000 K when the methane concentration is increased to 4.2 vol.%.

In the experiment, the methane and hydrogen feed is always switched off as soon as the temperature exceeds approximately 1100 K to prevent damages of the catalyst and the equipment. Before light-off the temperature increases only slightly with increasing methane feed due to an increasing but small amount of reacting methane. However, this temperature increase seems to be large enough to reach a temperature at which light-off takes place. The light-off temperature of methane oxidation decreases with increasing hydrogen content as shown in Fig. 2. Furthermore, the temperature at which light-off occurs increases with increasing hydrogen feed. At a hydrogen feed between

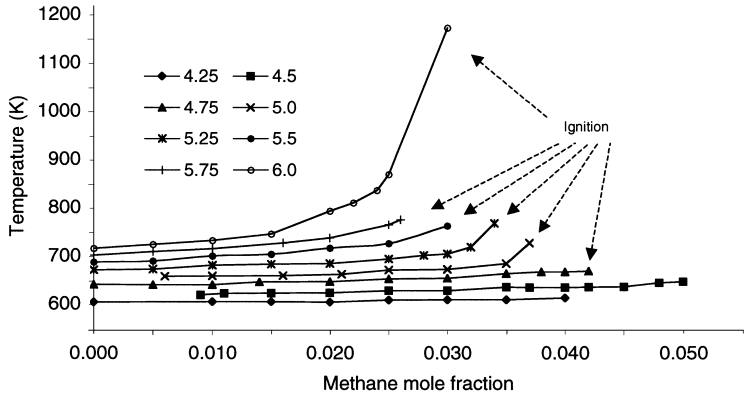

Fig. 2. Experimental measured temperature of the outlet gas as a function of inlet methane feed for several hydrogen additions. The runs always begin with low methane concentrations at the given amount of hydrogen addition; the methane concentration is slowly increased.

5 and 6 vol.%, the temperature increases stronger with rising methane concentration.

The hydrogen assisted catalytic light-off of methane is primarily determined by the catalyst temperature that is a result of the heat release due to catalytic hydrogen oxidation. So, higher hydrogen addition ensures light-off. Decreasing hydrogen addition requires increasing methane feed for light-off as expected from a former work, where the decrease of catalytic ignition temperatures with increasing methane/oxygen ratio is described [1].

It should be mentioned that the exact hydrogen concentrations, at which the light-off of catalytic methane combustion occurs, also depends on other parameters such as platinum loading, thermal insulation, and flow rate.

3. Modeling approach

Our approach to model catalytic combustion consists in coupling of the fluid flow and the chemical processes in the gas phase and at the gas–surface interface. The fluid flow is described by the Navier–Stokes equations, an energy conservation equation, and additional conservation equations for each chemical species. This equation system is closed by the ideal gas law. In the cases studied in this paper, the flow field is laminar.

Two flow configurations, the stagnation point flow onto a catalytic foil and the flow through a single channel with a catalytic inner surface, are numerically studied in the present work.

3.1. Stagnation flow configuration

In the stagnation flow configuration, a flow with uniform velocity distribution is imposed at a certain distance, 5 cm in the present study, from a flat catalytically active foil, as shown in Fig. 3. By confining the attention to the center of this foil, edge effects can be neglected, permitting use of the one-dimensional equations describing this system [3–5]. The dependent variables are density, momentum, temperature, and mass fraction of each gas phase species. These variables are independent of the radius and depend only on the distance from the foil (x) and on time.

The surface of the catalytic foil is described by its coverage with adsorbed species and its temperature. Here, the catalyst temperature is derived from an energy balance at the gas–surface interface including conductive, convective, and diffusive energy transport from/to the gas phase, chemical heat release by surface reactions, thermal radiation, and catalyst heat capacity. The variation of the surface coverage is calculated from surface reaction rates. A transient one-dimensional computer program, developed previously [1], is used to solve the resulting equation system. The time-dependent profiles of density, velocity, temperature, and species concentrations as a function of the distance from the catalyst as well as the surface coverage and the catalyst temperature are calculated.

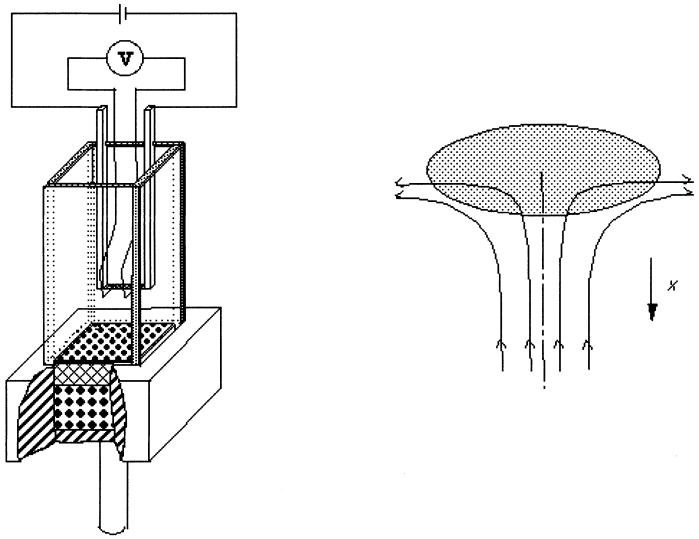

Fig. 3. Typical experimental setup to study catalytic combustion in a stagnation flow configuration (left, [6]) and sketch of the model as used in the present paper (right).

3.2. Single channel configuration

Honeycomb monoliths, as proposed for gas turbine applications, consist of thin channels with inner catalytic surface and diameters of the order of 1 mm. It can often be assumed that every channel of the monolith behaves essentially alike, so radial profiles over the monolith can be neglected. Therefore, we study only one single channel as shown in Fig. 4. In the model, the shape of the channel is assumed to be cylindrical which permits the use of a two-dimensional axi-symmetric description of the flow field. The Navier–Stokes equations have to be solved with the axial and radial spatial coordinates as independent variables.

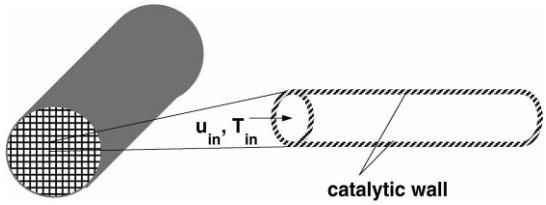

Fig. 4. Sketch of a monolith structure and an enlarged view of the individual channel as used in the simulation. Note, the channel diameter (1.8 mm) is much smaller than the channel length (50 mm).

This problem is simulated using the computational fluid dynamics code FLUENT [7] which is coupled to external subroutines that model the surface chemistry [8]. These subroutines calculate the mass fluxes at the wall due to surface reactions and the surface coverage with species adsorbed. The temperature is derived from the governing equation for enthalpy, also including chemical heat release and heat transport in the channel wall.

3.3. Surface chemistry

The chemical processes on the surface are described by a set of elementary reactions. Seven gas phase species (CH_4, O_2, H_2, H_2O, CO, CO_2, N_2) are included in the model, of which nitrogen is a chemically inert species. Eleven *surface species* (H(s), O(s), OH(s), H_2O(s), C(s), CO(s), CO_2(s), CH_3(s), CH_2(s), CH(s), Pt(s)) describe the coverage of the surface with adsorbed species. Here, Pt(s) denotes the uncovered surface site fraction that is available for adsorption.

Both gas phase species and surface species can be produced and depleted by surface reactions. The production rate $\dot{s}_i$ for each species is written as

$$\dot{s}_i = \sum_{k=1}^{K_s} \nu_{i_k} k_{f_k} \prod_{i=1}^{N_g+N_s} [X_i]^{\nu'_{i_k}}. \quad (1)$$

Table 1
Surface reaction mechanism[a]

	A	β	E_a	ε_i, μ_i[b]
(1) H_2+2Pt(s) ⇒ 2H(s)	4.60×10^{-2}			$\mu_{Pt(s)} = -1$[c]
(2) 2H(s) ⇒ 2Pt(s) + H_2	$3.70\times10^{+21}$	0.0	67.4	$\varepsilon_{H(s)} = 6$
(3) H + Pt(s) ⇒ H(s)	1.00			[c]
(4) O_2+2Pt(s) ⇒ 2O(s)	$1.80\times10^{+21}$	−0.5	0.0	
(5) O_2+2Pt(s) ⇒ 2O(s)	2.30×10^{-2}			[c]
(6) 2O(s) ⇒ 2Pt(s) + O_2	$3.70\times10^{+21}$	0.0	213.2	$\varepsilon_{O(s)} = 60$
(7) O + Pt(s) ⇒ O(s)	1.00			[c]
(8) H_2O + Pt(s) ⇒ H_2O(s)	0.75			[c]
(9) H_2O(s) ⇒ H_2O + Pt(s)	$1.00\times10^{+13}$	0.0	40.3	
(10) OH + Pt(s) ⇒ OH(s)	1.00			[c]
(11) OH(s) ⇒ OH + Pt(s)	$1.00\times10^{+13}$	0.0	192.8	
(12) O(s) + H(s) ⇔ OH(s) + Pt(s)	$3.70\times10^{+21}$	0.0	11.5	
(13) H(s) + OH(s) ⇔ H_2O(s) + Pt(s)	$3.70\times10^{+21}$	0.0	17.4	
(14) OH(s) + OH(s) ⇔ H_2O(s) + O(s)	$3.70\times10^{+21}$	0.0	48.2	
(15) CO + Pt(s) ⇒ CO(s)	8.40×10^{-1}			$\mu_{Pt(s)} = +1$[c]
(16) CO(s) ⇒ CO + Pt(s)	$1.00\times10^{+13}$	0.0	125.5	
(17) CO_2(s) ⇒ CO_2+Pt(s)	$1.00\times10^{+13}$	0.0	20.5	
(18) CO(s) + O(s) ⇒ CO_2(s) + Pt(s)	$3.70\times10^{+21}$	0.0	105.0	
(19) CH_4+2Pt(s) ⇒ CH_3(s) + H(s)	1.00×10^{-2}			$\mu_{Pt(s)} = +0.3$[c]
(20) CH_3(s) + Pt(s) ⇒ CH_2(s) + H(s)	$3.70\times10^{+21}$	0.0	20.0	
(21) CH_2(s) + Pt(s) ⇒ CH(s) + H(s)	$3.70\times10^{+21}$	0.0	20.0	
(22) CH(s) + Pt(s) ⇒ C(s) + H(s)	$3.70\times10^{+21}$	0.0	20.0	
(23) C(s) + O(s) ⇒ CO(s) + Pt(s)	$3.70\times10^{+21}$	0.0	62.8	
(24) CO(s) + Pt(s) ⇒ C(s) + O(s)	$1.00\times10^{+18}$	0.0	184.0	

[a] The units of A are given in terms of mol, cm, and s. E_a and ε_i are in kJ mol^{-1}. Reactions (4) and (5) represent alternative competing pathways.
[b] According to Eq. (2).
[c] Sticking coefficient.

Here, K_s is the total number of elementary surface reactions (including adsorption and desorption), v_{i_k}, v'_{i_k} are stoichiometric coefficients (right minus left side of reaction equation, left side), k_{f_k} the forward rate coefficient, and $[X_i]$ is the concentration of species i. For adsorbed species, the concentrations are given in mol cm^{-2}. N_g is the number of gas phase species and N_s is the number of surface species. The rate coefficients of adsorption, desorption, and surface reactions can also depend on surface coverage leading to the following rate expression for the rate coefficient of the forward reaction k:

$$k_{f_k} = A_k T^{\beta_k} \exp\left[\frac{-E_{a_k}}{RT}\right] \prod_{i=1}^{N_s} \Theta_i^{\mu_{i_k}} \exp\left[\frac{\varepsilon_{i_k}\Theta_i}{RT}\right] \quad (2)$$

with A_k as pre-exponential factor, β_k as temperature exponent, and E_{a_k} as activation energy of reaction k. Coefficients μ_{i_k} and ε_{i_k} describe the dependence of the rate coefficients on the surface coverage, Θ_i, of species i.

The variation of the surface coverage that is the fraction of surface sites covered by species i is calculated from surface reaction rates according to

$$\frac{\partial\Theta_i}{\partial t} = \frac{\dot{s}_i}{\Gamma} \quad (i = N_g + 1, \ldots, N_g + N_s), \quad (3)$$

where Γ is the surface site density of the catalyst. The value of 2.72×10^{-9} mol cm^{-2} is used for the platinum catalyst in this study.

The reaction scheme shown in Table 1 was developed to model ignition of catalytic hydrogen, carbon monoxide, and methane combustion [1,6,9–11] and is used here without modification. In the present study, gas phase reactions are not taken into account. However, both numerical codes are also capable of using large gas phase reaction mechanisms.

4. Numerical results

4.1. Stagnation flow simulations

Methane/hydrogen/air mixtures flow slowly at atmospheric pressure onto the platinum foil. The inlet velocity is 1 m s^{-1}, and the inlet temperature is always 300 K. The temperature of the catalytic foil (T_{cat}) is derived from the energy balance at the foil, so the heat release by the exothermic combustion reaction leads to an increase of foil temperature T_{cat}. Because this energy balance also includes heat conduction into the gas phase, inlet velocity variation leads to variation of the foil temperature.

We start our simulation with a H_2/air mixture with a constant amount of H_2 in air. The hydrogen is reacting on the catalyst surface. This procedure follows the experimental one discussed above. Depending on the hydrogen concentration, between 2.5 and 4.0 vol.% for the results shown in Fig. 5, the resulting catalyst temperature is between 708 and 978 K. Now, methane is added to the inlet gas. The temperature stays almost constant, it even decreases a bit for low hydrogen concentration, as shown for 2.5 vol.% H_2 in Fig. 5 (top). For higher initial hydrogen concentration, e.g. 3.0 vol.% in Fig. 5, the catalyst temperature increases only slightly at low methane concentration, and only a small amount of methane is consumed. However, this small temperature rise eventually leads to light-off of methane combustion at 4.2 vol.% methane addition. A further rise of methane concentration steadily increases the catalyst temperature due to the increasing amount of methane oxidized on the catalyst. Increasing hydrogen concentrations lead to less methane needed for light-off. At 4 vol.% H_2 in the initial mixture, the hydrogen oxidation provides enough heat to have a catalyst temperature at which the light-off of the methane oxidation reaction is independent of methane concentration; all the methane is consumed, even at very low methane concentration.

Even though the flow configuration simulated completely differs from that used in the experiment, the qualitative features observed are predicted well. This agreement can be explained by the fact that the light-off process itself is kinetically controlled. Here, we really benefit from using elementary-step reaction mechanisms to model the surface chemistry.

Fig. 6 reveals the transient behavior of the catalytic system during the onset of heterogeneous methane

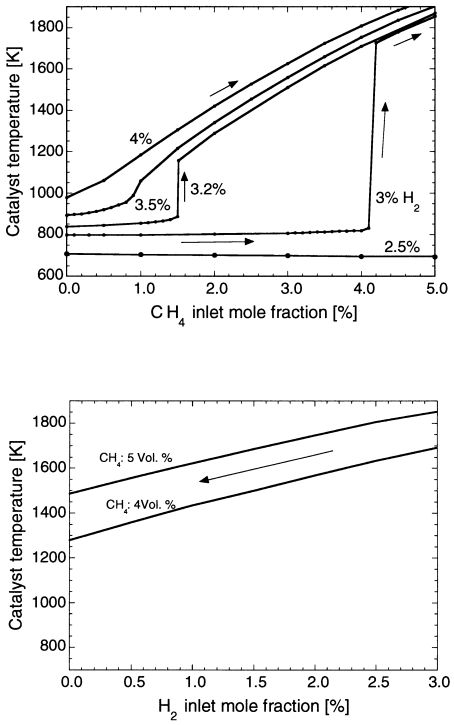

Fig. 5. Calculated catalyst temperatures versus methane mole fraction for CH_4/H_2/air inlet mixtures with constant H_2 addition (top) and versus hydrogen mole fraction for a CH_4/H_2/air inlet mixture with constant 4 and 5 vol.% CH_4 after methane combustion light-off (bottom).

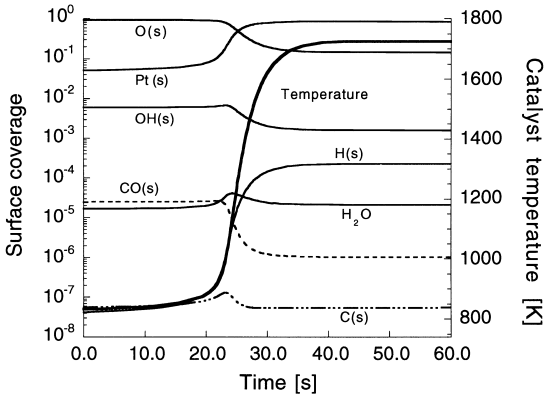

Fig. 6. Variation of surface coverage and catalyst temperature during light-off of methane combustion. At time zero, the inlet methane concentration in the total mixture (3 vol.% H_2 in air) is increased from 4.1 to 4.2 vol.%.

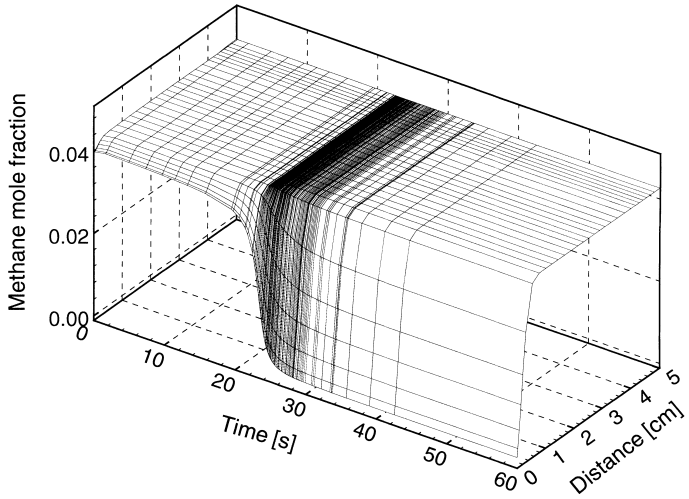

Fig. 7. Temporal variation of methane profiles in the gas phase as a function of time and distance from the catalytic foil during light-off of heterogeneous methane combustion with 3 vol.% H_2 in the air. The time is zero at the time at which the methane concentration is increased from 4.1 to 4.2 vol.%.

combustion for the case of 3 vol.% H_2 addition. The temporal profiles of catalyst temperature and surface coverage with adsorbed species are shown. The time is zero when the methane mole fraction is increased from 4.1 to 4.2 vol.%. In the beginning, the surface is mainly covered with oxygen that is in excess in the inlet mixture. The large oxygen coverage inhibits methane adsorption and subsequent methane oxidation. The sticking coefficient of hydrogen is about four times larger than that of methane. Hence, almost all the uncovered surface sites (Pt(s)) available for adsorption will primarily be used for hydrogen adsorption. Therefore, hydrogen is completely depleted, but only a small amount of methane is consumed. However, this small amount of methane consumption leads to a slight temperature increase when the methane concentration is risen as shown in Fig. 5 (top). The adsorption–desorption equilibrium of oxygen slowly shifts towards desorption with increasing temperature. When the catalyst reached a critical temperature, here 800 K, the number of uncovered surface sites (Pt(s)) is large enough to allow a sufficiently large number of methane molecules to adsorb. The subsequent exothermic oxidation of methane and fast desorption of products lead to a further temperature increase and a more and more uncovered surface; light-off of methane oxidation occurs. During this process the surface coverage strongly varies, eventually leading to over 80% uncovered surface sites (Pt(s)).

Prior to light-off, methane combustion is kinetically controlled, after ignition the system is transport limited. This transient behavior is clearly revealed in Fig. 7, where large gradients of methane concentration are formed close to the catalytic foil.

After ignition, the hydrogen feed can be reduced without extinction as shown in Fig. 5 (bottom). In the two cases shown, we start with an ignited mixture, keep the methane mole fraction constant at 4 and 5 vol.%, respectively, and decrease the hydrogen feed. The 4 vol.% case is started from the ignited 4.2 vol.% situation by reduction of methane feed before the hydrogen concentration is decreased. Even without any hydrogen addition the mixtures keep ignited at the chosen conditions. The mixture also keeps ignited when the methane concentration is lowered to a value that is lower than that necessary for ignition as shown by the 4% curve.

The decisive point in hydrogen assisted catalytic ignition is that hydrogen oxidation can easily lead to a temperature at which methane oxidation starts. However, hydrogen addition may result in temperatures that become too high for the catalyst and the surrounding technical devices.

4.2. Single channel simulations

The conditions in the simulation follow the experimental setup: the diameter of the single channel is 1.8 mm, and the length of the channel is 5 cm. The CH_4/H_2/air mixture flows with a uniform inlet velocity of 0.8 m s^{-1} at atmospheric pressure (1 bar) and at 300 K into the channel. In the experiment, the inner surface of the channel has Pt dispersed on a wash coat. However, in the model, Pt is uniformly dispersed on the inner channel wall.

In contrast to the time resolved stagnation flow simulation, the steady state is now simulated, that means the transient behavior during ignition is not resolved.

The amounts of methane and hydrogen is varied in the inlet mixture. Without hydrogen addition, no significant amount of methane is converted, and the catalyst temperature remains at 300 K at these conditions. The catalytic surface is covered with oxygen inhibiting the adsorption and subsequent reaction of methane.

When a lean hydrogen/air mixture is fed, the catalyst ignites and all the hydrogen is consumed leading to a rapid temperature increase of the monolith. The reaction starts immediately at the catalyst entrance and hydrogen is completely consumed within few millimeters. At steady state, the catalyst temperature equals the adiabatic temperature. After hydrogen is ignited, methane is added. If the catalyst temperature is lower than approximately 750 K, because the heat loss is too large or the initial hydrogen mixture is too lean, the onset of methane combustion depends on the methane concentration fed. The catalyst temperature slowly increases with increasing methane/air ratio until the ignition of methane combustion occurs leading to a jump of the catalyst temperature. This behavior is similar to that discussed above for the stagnation flow configuration. If the catalyst temperature is high enough (over 800 K for the conditions used here), light-off of methane combustion will occur immediately. In this case, all the CH_4 is completely consumed even for very low methane concentrations.

Because of heat loss in the experiment, which is neglected in the simulation, the temperatures measured are lower than the calculated values. Consequently, the mixture compositions, at which methane combustion starts, differ in experiment and simulation.

Fig. 8 shows the simulation results for the following conditions: 4 vol.% CH_4 in air with 6 vol.% H_2 addition. All the methane and hydrogen is completely consumed within the first few millimeters of the catalyst channel. Also here, some CO is formed at the catalytic surface and diffuses into the gas phase. However, almost all the carbon monoxide is consumed by surface reactions again, farther downstream.

5. Summary and conclusions

The addition of hydrogen to the initial mixture offers a way to light-off catalytic combustion of methane on platinum. It seems that the main effect of hydrogen addition is to provide enough heat to reach a catalyst temperature at which methane oxidation will light-off. A consequence is that hydrogen addition must be over a certain minimum, 3 vol.% in our case, in order to be able to use lean methane/air mixtures. The temperature of light-off of methane combustion also depends on methane concentration and is in all cases investigated above 600 K. An increase of the methane concentration will generally support light-off. The high temperatures reached after light-off may affect the function of the catalytic monolith itself or the surrounding equipment. We currently investigate the influence of preheat on methane light-off to understand if hydrogen addition also leads to kinetic effects aside from supplying heat.

The light-off behavior can be explained by the kinetic processes on the catalyst surface. The oxygen coverage of the platinum surface inhibits methane oxidation at low temperatures. The two-dimensional simulation of a single channel of the honeycomb monolith reveals the interaction of mass and heat transport and surface chemistry. After light-off, all the reactants are consumed within the first few millimeters of the monolith. Gas phase reactions have not been incorporated into the simulation yet. However, the computational tools are principally capable of taking detailed gas phase reaction mechanisms into account.

To summarize, in this paper we show that one-dimensional stagnation flow simulations are able to capture the essential physics of hydrogen assisted catalytic combustion such as hysteresis with respect to the amount of hydrogen added to the system or the danger of damage to the catalyst by the rapid increase in temperature at certain critical hydrogen concentra-

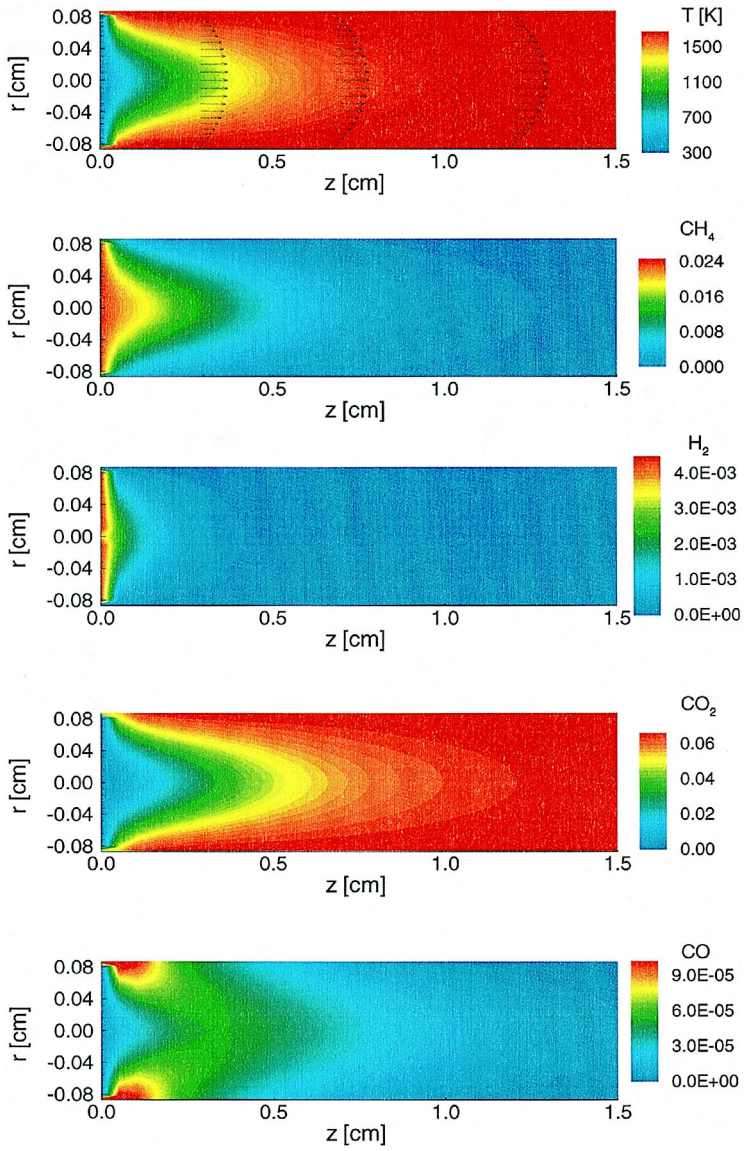

Fig. 8. Calculated profiles of temperature (velocity vectors plotted on top) and mass fractions of CH_4, H_2, CO_2, and CO in a single channel; 4 vol.% CH_4, 6 vol.% H_2 in air. For visual clarity, the radial coordinate has been enlarged and only the entrance region of the channel is shown.

tions. Furthermore, the first series of two-dimensional calculations of the flow through a single channel of the catalyst shows the feasibility of reproducing the experiment in a numerical simulation which can be run on a standard desktop workstation. Therefore, the mutual benefit of experiments and modeling will be able to explain the results with respect to the kinetic behavior of species which cannot be measured in the experiments. Given the large parameter space (hydrogen concentration, methane concentration, initial temperature, flow rate, length of the catalyst), modeling and numerical simulations will help to reduce the number of runs of the experiments to map out the parameter range of interest.

Acknowledgements

Two of the authors (OD and UR) would like to thank Professor J. Warnatz, University of Heidelberg, for his continuous support. L.I. Maier gratefully acknowledges a grant from the Otto–Benecke–Stiftung eV for a 1-year stay at the Interdisciplinary Center of Scientific Computing (IWR) at University of Heidelberg.

References

[1] O. Deutschmann, R. Schmidt, F. Behrendt, J. Warnatz, in: Proceedings of the 26th International Symposium on Combustion, The Combustion Institute, Pittsburgh, PA, 1996, pp. 1747–1754.
[2] G. Veser, L.D. Schmidt, AIChE J. 42 (1996) 1077–1087.
[3] G. Evans, R. Greif, ASME J. Heat Transfer 109 (1987) 928.
[4] R.J. Kee, J.A. Miller, G.A. Evans, G.H. Dixon-Lewis, in: Proceedings of the 22nd International Symposium on Combustion, The Combustion Institute, Pittsburgh, PA, 1988, p. 1479.
[5] J. Warnatz, M.D. Allendorf, R.J. Kee, M.E. Coltrin, Combust. Flame 96 (1994) 393.
[6] F. Behrendt, O. Deutschmann, R. Schmidt, J. Warnatz, in: B.K. Warren, S.T. Oyama (Eds.), Heterogeneous Hydrocarbon Oxidation, ACS Symposium Series, Vol. 638, Washington, 1996, p. 48 (Chapter 4).
[7] FLUENT 4.4, Fluent, Lebanon, NH, 1997.
[8] O. Deutschmann, L.D. Schmidt, AIChE J. 44 (1998) 2465–2477.
[9] D.A. Hickman, L.D. Schmidt, AIChE J. 39 (1993) 1164.
[10] O. Deutschmann, F. Behrendt, J. Warnatz, Catal. Today 21 (1994) 461.
[11] M. Rinnemo, O. Deutschmann, F. Behrendt, B. Kasemo, Combust. Flame 111 (1997) 312–326.